Two-Dimensional Super-Resolution Direction Finding Algorithm for Wideband Chirp Signals

Baoyu Guo and Jiaqi Zhen(✉)

College of Electronic Engineering,
Heilongjiang University, Harbin 150080, China
zhenjiaqi2011@163.com

Abstract. Conventional direction finding algorithms for wideband signal need to preliminarily estimate the Direction of Arrival (DOA) and power of the noise roughly, and it has large focusing error. In order to solve these problems, a super-resolution direction finding algorithm for two dimensional (2-D) wideband chirp signals is proposed, the Fractional Fourier Transform (FRFT) is applied to focus the energy of the signals in every frequency by the rotational characteristic of FRFT, then algorithm for narrowband signals is used to estimate the DOA, computer simulation results prove the effective of the algorithm.

Keywords: Wideband signals · Chirp signals · Direction of Arrival · Fractional Fourier Transform

1 Introduction

Spatial spectrum estimation algorithms are widely used in the fields of radar and mobile communication, but most of them are only adapt to the narrowband signals, that is the band of signal is far less than its center frequency, the signal envelope on every sensors is seem to be the same. But wideband signals are abounding in practical [1], it has been widely researched in recent years [2–5], one of them is Chirp signal. Generally speaking, algorithms of wideband signals are divided into two types: one is incoherent signal subspace method (ISM) [6], the other is coherent signal subspace method (CSM) [7, 8], the latter can deal with coherent signals, so it is obtained extensive research, its basic idea is to focus signal spaces of different frequencies to the reference frequency point, then we can get the covariance matrix of a single frequency, but it often needs to preliminarily estimate the DOA and power of the noise roughly, and it has a large focusing error. In this paper, focusing matrix is constructed by method of FRFT, then we estimate two-dimensional DOA of signals, wherever compare its performance with TCT algorithm.

This work was supported by the National Natural Science Foundation of China under Grant 61501176, Natural Science Foundation of Heilongjiang Province F2018025, University Nursing Program for Young Scholars with Creative Talents in Heilongjiang Province UNPYSCT-2016017, the postdoctoral scientific research developmental fund of Heilongjiang Province in 2017 LBH-Q17149.

S. Liu and G. Yang (Eds.): ADHIP 2018, LNICST 279, pp. 151–159, 2019.
https://doi.org/10.1007/978-3-030-19086-6_17

2 Signal Model

FRFT is a special formation of Fourier Transform, it is also related to rotation of the Wigner distribution of the given signal, it can be written

$$X_P(u) = \{F_P[x(t)]\} = \int_{-\infty}^{+\infty} x(t)K_P(t,u)\mathrm{d}t \tag{1}$$

where parameter p is called the fractional order of the transform, $F_P[\cdot]$ is kernel-based integral transformation of the form, the transform kernel $K_P(t,u)$ is

$$K_P(t,u) = \begin{cases} \sqrt{\frac{1-\mathrm{j}\cot\alpha}{2\pi}}\exp\left(\mathrm{j}\frac{t^2+u^2}{2}\mathrm{ctg}\alpha - \mathrm{j}ut\csc\alpha\right), \alpha \neq n\pi \\ \delta(t-u), \alpha = 2n\pi \\ \delta(t-u), \alpha = (2n\pm 1)\pi \end{cases} \tag{2}$$

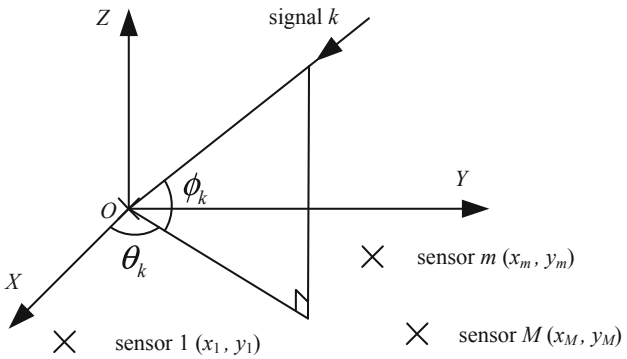

Fig. 1. Model of the signal.

As shown in Fig. 1, consider N chirp wideband signals emitted from the far field impinging on plane array of M sensors ($N < M$), arrange of the sensors is arbitrary, the phase reference point is the origin of coordinate, expression of chirp signals received by reference point is

$$s_0(t) = \exp\left[\mathrm{j}\pi\left(2f_0t^2 + kt\right)\right] \tag{3}$$

where f_0 is the initial frequency and k is the frequency modulation rate, we can obtain FRFT of the Eq. (2):

$$F_{\alpha s_0}(u) = \rho\exp\left[\mathrm{j}\frac{u^2(2k\cos\alpha - \sin\alpha) + 4\pi f_0 u - 4\pi^2 f_0^2\sin\alpha}{2(2k\sin\alpha + \cos\alpha)}\right] \tag{4}$$

where $\rho=\sqrt{\frac{\cos\ \alpha+\mathrm{j}\sin\ \alpha}{\cos\ \alpha+2k\ \sin\ \alpha}}$, use FRFT on the chirp signals $x_m(t)$ received by mth sensor, that is

$$F_{\alpha x_m}(u)=F_{\alpha s_0}(u)\exp\left[\mathrm{j}\frac{2k\tau_m^2\cos\ \alpha-4ku\tau_m-4\pi f_0\tau_m\cos\ \alpha}{2(\cos\ \alpha+2k\ \sin\ \alpha)}\right]+F_{\alpha N}(u) \tag{5}$$

where τ_m is the delay time to the reference sensor when the chirp signal arriving at the mth sensor, and $\tau_m=\frac{x_m\cos\ \varphi\ \cos\ \theta+y_m\sin\ \varphi\ \cos\ \theta}{c}$, φ, θ is separately the azimuth and elevation of the two-dimensional signal, c is speed of light, $F_{\alpha N}$ is FRFT of white Gaussian noise, the array manifold can be reduced from Eq. (4):

$$\boldsymbol{a}(u,\alpha)=\left\{\begin{array}{l}\exp\left[\mathrm{j}\frac{2k\tau_1^2\cos\ \alpha-4ku\tau_1-4\pi f_0\tau_1\cos\ \alpha}{2(\cos\ \alpha+2k\ \sin\ \alpha)}\right],\\ \cdots,\exp\left[\mathrm{j}\frac{2k\tau_m^2\cos\ \alpha-4ku\tau_m-4\pi f_0\tau_m\cos\ \alpha}{2(\cos\ \alpha+2k\ \sin\ \alpha)}\right]\end{array}\right\}^{\mathrm{T}} \tag{6}$$

so it is affected by the parameters of the chirp signal, output of the array is defined as:

$$\boldsymbol{X}(u,\alpha)=\boldsymbol{A}(u,\alpha)\boldsymbol{S}(u,\alpha)+\boldsymbol{N}(u,\alpha) \tag{7}$$

where

$$\boldsymbol{S}(u,\alpha)=[s_1(u,\alpha),\cdots s_N(u,\alpha)]^{\mathrm{T}} \tag{8}$$

it is the vector of the signal, and

$$\boldsymbol{N}(u,\alpha)=[n_1(u,\alpha),\cdots,n_M(u,\alpha)]^{\mathrm{T}} \tag{9}$$

it is the vector of the noise, then matrix of array manifold in FRFT domain can be expressed as:

$$\boldsymbol{A}(u,\alpha)=[\boldsymbol{a}(u,\alpha,\theta_1,\varphi_1),\cdots,\boldsymbol{a}(u,\alpha,\theta_N,\varphi_N)] \tag{10}$$

mathematical expectation of Eq. (4) can be written

$$E\left[F_{\alpha X_m}(u)F_{\alpha X_m}^{\mathrm{H}}(u)\right]=|F_{\alpha s_0}(u)|^2+|F_{\alpha N}(u)|^2 \tag{11}$$

where $E[.]$ denotes mathematical expectation, and

$$|F_{\alpha s_0}(u)|^2=\left|\frac{1}{\cos\ \alpha+2\pi k\ \sin\ \alpha}\right| \tag{12}$$

so we can obtain the FRFT covariance matrix of $\boldsymbol{X}$

$$\boldsymbol{R}_X(u)=E\left[\boldsymbol{X}(u)\boldsymbol{X}^{\mathrm{H}}(u)\right] \tag{13}$$

3 Focusing Energy of the Signals

In order to focus the energy of the signals, we need to estimate their frequencies, from Eq. (12), we have

$$\mathrm{ctg}\alpha = -k \tag{14}$$

where k is frequency modulation rate of chirp signal, combine Eqs. (6) and (14), we have

$$\begin{aligned}\boldsymbol{a}(u,\alpha,\theta) = \{&\exp[\mathrm{j}(\mathrm{ctg}\alpha\tau_1 + 2ku\ \sec\ \alpha + 2\pi f_0)\tau_1], \cdots, \\ &\exp[\mathrm{j}(\mathrm{ctg}\alpha\tau_m + 2ku\ \sec\ \alpha + 2\pi f_0)\tau_m]\}^{\mathrm{T}}\end{aligned} \tag{15}$$

steer vectors can be deduced from Eq. (15), it is easer than Eq. (5), computation is decreased obviously, then spatial spectrum can be obtained by the equation below:

$$P(\theta,\varphi) = \frac{1}{\mathbf{a}^{\mathrm{H}}(u,k,\theta,\varphi)\mathbf{R}^{-1}\mathbf{a}(u,k,\theta,\varphi)} \tag{16}$$

When estimating the directions of one signals reflecting from multipath, we only need to know one modulation rate of them, as they are the same. The algorithm of the paper has two properties: (1) It does not need to preliminarily estimate DOA and the power of the noise roughly; (2) It focuses the energy of chirp signal by FRFT, so as to enhance the signal to noise ratio, the algorithm of the paper is summarized as follows:

Step 1: Determine frequency modulation rate k of chirp signal;
Step 2: Calculate the steer vectors matrix by FRFT;
Step 3: Collect data, form the correlation matrix $\mathbf{R}_X(u)$ by Eq. (13);
Step 4: Evaluate $P(\theta,\phi)$ versus θ, φ with (16).

4 Simulations

In order to verify the validity of the method in this paper and to compare the performance with other algorithms, some experiments with matlab are presented, in the experiment, without loss of generality, we consider an arbitrary plane array of 8 sensors, the coordinates are given by (0,0), (−0.16,0.12), (−0.049,0.086), (−0.22,0.055), (−0.079,−0.032), (0.065,0.13), (0.08,0.24), (0.037,−0.044), unit is meter. Some Chirp signals come from the same source, the frequency ranges from 4 GHz to 6 GHz, we separately use TCT algorithm and method in this paper to estimate DOA, FFT and FRFT is used in each snapshot to sample the frequency spectrum of the signals at 33 points, and take 100 times snapshots in every frequency.

Simulation 1 Spatial Spectrum
Consider two chirp signals arriving from directions $(56°, 65°)$, $(66°, 75°)$, $(74°, 83°)$ respectively, SNR is 12 dB, Figs. 2 and 3 have shown the spatial spectrum of TCT-MVDR and algorithm of the paper. As seen from Figs. 2 and 3, by the course of

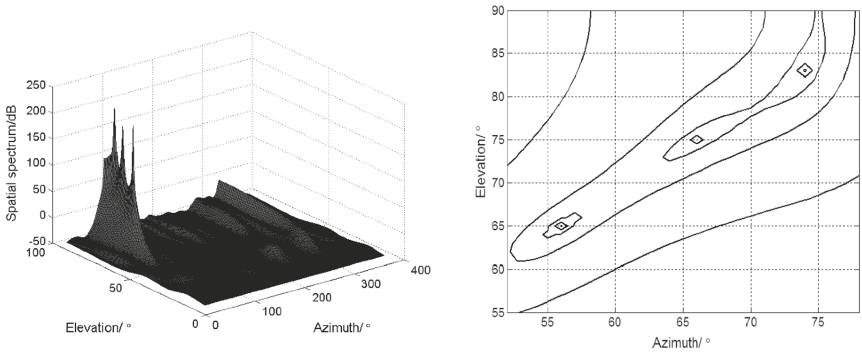

(a) Spatial spectrum (b) Projection of the spectrum

Fig. 2. Spatial spectrum of TCT-MVDR.

focusing in FRFT domain, the spatial spectrum peak of algorithm of the paper is sharper than that of the TCT-MVDR.

Simulation 2 Precision of This Algorithm

Consider four far-field chirp signals arriving at the sensors from $(35°, 50°)$, $(45°, 60°)$, $(55°, 70°)$, $(65°, 80°)$ with same power, SNR varies from −5 dB to 15 dB, step size is 1 dB, 600 times Monte-Carlo trials have run for each SNR, the average of them is regarded as the measure result for this SNR. In order to describe the angle measurement accuracy, Root Mean Squared Error (RMSE) of two-dimensional angle measurement is defined as:

$$\text{RMSE} = \sum_{i=1}^{4} \sqrt{(\hat{\phi}_i - \phi_i)^2 + (\hat{\theta}_i - \theta_i)^2} \qquad (i = 1, 2, 3, 4) \tag{17}$$

ϕ_i and $\theta_i (i = 1, 2, 3, 4)$ are respectively the true values of azimuth and elevation of the ith signal, $\hat{\phi}_i$ and $\hat{\theta}_i$ are separately the values estimated, Fig. 4 shows the RMSE of two algorithms versus SNR.

From Fig. 4 it is seen that RMSE of TCT-MVDR is larger than that of algorithm of the paper, when SNR is higher than 13 dB, RMSE of TCT-MVDR is zero, but that of algorithm of the paper is zero when SNR is 9 dB.

Simulation 3 Resolution Capability

Consider two signals respectively arriving from directions $(56°, 65°)$, $(56°, 70°)$, SNR is 6 dB, Figs. 5 and 6 have shown the spatial spectrum of TCT-MVDR and algorithm of the paper. From Figs. 5 and 6 we know when the signals are close, TCT-MVDR can not distinguish them, but algorithm of the paper can distinguish them at this moment.

Consider two chirp signals arriving at the sensors, in order to be convenient, the incident angle (ϕ, θ) is replaced by ϑ, resolving power boundary is generally defined that the peak of mean value of angles of two signals is equal to the mean peak value of two signals for spatial spectrum algorithm, that is

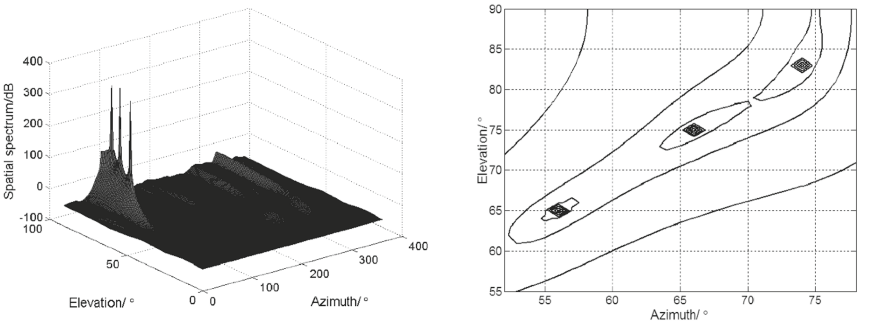

(a) Spatial spectrum (b) Projection of the spectrum

Fig. 3. Spatial spectrum of algorithm of the paper.

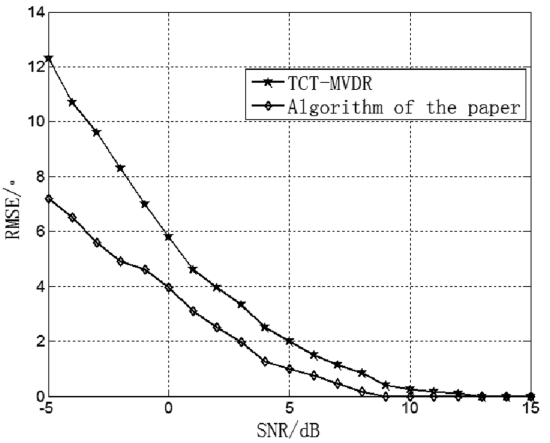

Fig. 4. The RMSE of three algorithms versus SNR.

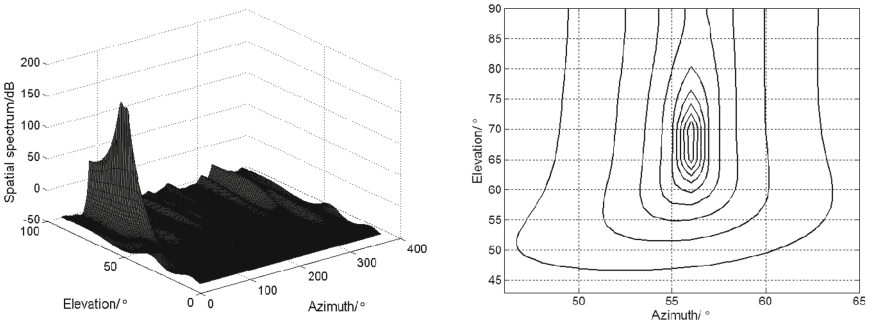

(a) Spatial spectrum (b) Projection of the spectrum

Fig. 5. Resolution capability of TCT-MVDR.

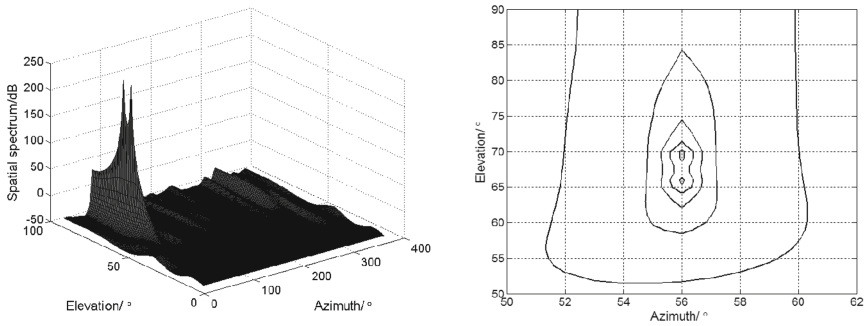

(a) Spatial spectrum (b) Projection of the spectrum

Fig. 6. Resolution capability of algorithm of the paper.

$$P(\vartheta_m) = P_{\text{peak}} \tag{18}$$

where $\vartheta_m = (\vartheta_1 + \vartheta_2)/2$ is the mean value of two signals; $P(\vartheta_m)$ is the peak of that; P_{peak} is mean peak value of two signals, and the following equality is satisfied

$$P_{\text{peak}} = \frac{1}{2}[P(\vartheta_1) + P(\vartheta_2)] \tag{19}$$

In the course of searching spectrum peaks, if there is hollow between two spectrum functions of the signals, namely left of the Eq. (18) is less than the right, it is thought that the two signals can be resolved; if not, they can not be resolved. Resolution capability is defined as:

$$\gamma(\Delta) = 1 - \frac{2\left|F\left(\frac{\Delta}{2}\right)\right|^2}{1-|F(\Delta)|^2} \cdot \left\{1 - |F(\Delta)| \cos[\varphi_{F(\Delta)} - 2\varphi_{F(\Delta/2)}]\right\} \tag{20}$$

where

$$F(\Delta) = \frac{1}{M}\sum_{i=1}^{M} \exp\left\{-j\frac{2\pi}{\lambda}(x_i \cos\,\phi + y_i \sin\,\phi) \times (\cos\,\theta_2 - \cos\,\theta_1)\right\} \tag{21}$$

We can know $\gamma(\Delta)$ can be defined as the measuring standard of resolution capability of two incident signals, the size of $\gamma(\Delta)$ is represented as degree of concavity between two spectrum peaks, the larger $\gamma(\Delta)$ is, the greater the degree of concavity is, the more power the resolution capability for two incident signal with space Δ is.

Consider two signals arriving at the sensors, their azimuths are both 45°, their elevations are taken 75° as point of symmetry, 600 times Monte-Carlo trials have run for each Δ, the average of them is regarded as the measure result for this Δ, here, we

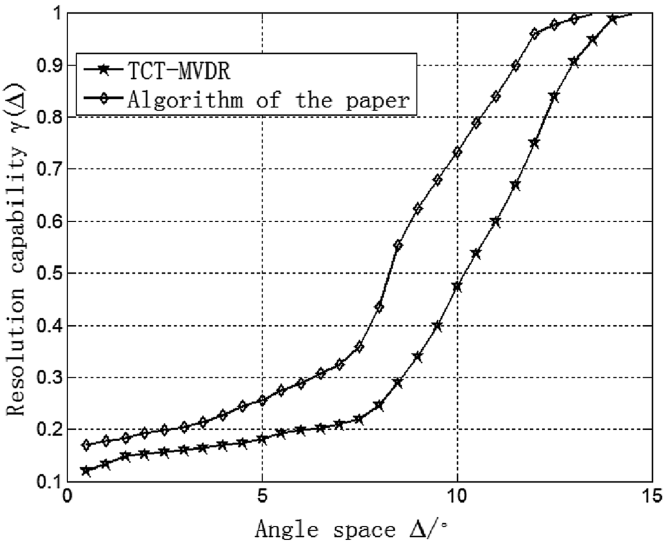

Fig. 7. Resolution capability of two algorithms with different angle spaces.

present the simulation result for resolution capability of two algorithms with different angle spaces, it is shown in Fig. 7.

From Fig. 7 it is seen the resolution capability of algorithm of the paper is better, as angle space increases, both of them are improving.

5 Conclusion

In this paper, we have used a kind of 2-D DOA estimation algorithm based on FRFT, it changes DOA estimation for wideband signals to that of narrowband signals, wherever, the energy of Chirp signal is more concentrative than in time-frequency, the performance of precision and resolution capability have been better.

References

1. Vinci, G., Barbon, F., Laemmle, B.: Wide-range, dual six-port based direction-of-arrival detector. In: 2012 Proceedings of Microwave Conference, Ilmenau, Germany, pp. 1–4 (2012)
2. Choliz, J., Angela, H.S., Valdovinos, A.: Evaluation of algorithms for UWB indoor tracking. In: 2011 Proceedings of Positioning Navigation and Communication, Dresden, Germany, pp. 143–148 (2011)
3. Bell, K.L., Zarnich, R.E., Wasyk, R.: MAP-PF wideband multitarget and colored noise tracking. In: 2010 Proceedings of Acoustics Speech and Signal Processing, Texas, USA, pp. 2710–2713 (2010)

4. Raines, B.D., Rojas, R.G.: Wideband tracking of characteristic modes. In: 2011 Proceedings of the 5th European Conference on Antennas and Propagation, Rome, Italy, pp. 1978–1981 (2011)
5. William, S., Salil, B., Adam, H.: System-level noise of an ultra-wideband tracking system. In: 2012 Proceedings of the 11th International Conference on Information Science, Signal Processing and their Applications, Montreal, Canada, pp. 634–639 (2012)
6. Shen, B., Yang, R., Ullah, S., Kwak, K.: Linear quadrature optimization-based non-coherent time of arrival estimation scheme for impulse radio ultra-wideband systems. IET Commun. **4**(12), 1471–1483 (2010)
7. Wang, H., Kaveh, M.: Coherent signal-subspace processing for the detection and estimation of angles of arrival of multiple wide-band sources. IEEE Trans. Acoust. Speech Signal Process. **33**(4), 823–831 (1985)
8. Acharyya, R.: Multiple classification without model order estimation. In: 2012 Proceedings of OCEANS, Yeosu, South Korea, pp. 1–6 (2012)